

CORRELATIONS IN THE FAR INFRARED BACKGROUND

ZOLTAN HAIMAN

NASA/Fermilab Astrophysics Center

Fermi National Accelerator Laboratory, Batavia, IL 60510, USA, email: zoltan@fnal.gov

AND

LLOYD KNOX

Department of Astronomy and Astrophysics, University of Chicago, Chicago, IL 60637, USA, email:

knox@flight.uchicago.edu

Accepted for publication in ApJ

ABSTRACT

We compute the expected angular power spectrum of the cosmic Far Infrared Background (FIRB). We find that the signal due to source correlations dominates the shot-noise for $\ell \lesssim 1000$ and results in anisotropies with rms amplitudes ($\sqrt{\ell(\ell+1)C_\ell/2\pi}$) between 5% and 10% of the mean for $\ell \gtrsim 150$. The angular power spectrum depends on several unknown quantities, such as the UV flux density evolution, optical properties of the dust, biasing of the sources of the FIRB, and cosmological parameters. However, when we require our models to reproduce the observed DC level of the FIRB, we find that the anisotropy is at least a few percent in all cases. This anisotropy is detectable with proposed instruments, and its measurement will provide strong constraints on models of galaxy evolution and large-scale structure at redshifts up to at least $z \sim 5$.

Subject headings: cosmology: theory – cosmology: observation – cosmology: far infrared background – cosmic microwave background – galaxies: formation – galaxies: evolution

1. INTRODUCTION

The recent discovery of the cosmic Far Infrared Background (FIRB, Puget et al. 1996, Fixsen et al. 1998, Dwek et al. 1998, Schlegel et al. 1998, Lagache et al. 1999) and the determination of its spectrum creates the opportunity for a new probe of structure formation in the high-redshift universe (e.g. Guiderdoni et al. 1998, Blain et al. 1999a). One way of improving our understanding of this background is to observe the sky with deep exposures at high angular resolution, to determine the number counts of discrete sources (Hughes et al. 1998, Barger et al. 1998, Eales et al. 1999, Smail et al. 1997, Holland et al. 1998, Blain et al. 1999b, Barger et al. 1999, Puget et al. 1999), and the redshift distribution of the contributing sources (e.g. Barger et al. 1999b, Blain et al. 1999c). Observations with the Sub-millimetre Common User Bolometer Array (SCUBA) camera (Holland et al. 1998) have indeed identified point sources at $450\mu\text{m}$ and $850\mu\text{m}$, which account for a large fraction ($\gtrsim 25\%$) of the FIRB at these wavelengths. However, a conclusive identification of optical counterparts, or the determination of the redshifts of these sources are still made difficult by the lack of detailed spectral information, and the uncertainty in the SCUBA-determined positions.

A complimentary approach is to observe the background at relatively low angular resolution in the “confusion limit” with the aim of studying its statistical properties. Such analyses have proven fruitful in the context of the Cosmic Microwave Background (CMB), as well as for the optical (Vogeley 1997) and near-infrared (Jimenez & Kashlinsky 1997, Kashlinsky et al. 1997) backgrounds. The

aim of the present *Letter* is to predict the lowest-order statistical property of the FIRB, the two-point angular correlation function, using simplified models for the origin of the background flux. Our results demonstrate that under conservative assumptions, the correlations are measurable with *Planck*¹ and other future instruments, such as the balloon-borne *Far Infrared Background Anisotropy Telescope* (FIRBAT) proposed by the TopHat² group and the *Bolometric Large Aperture Sub-mm Explorer* (BLASE, Dragovan, M. 1999). In addition, the signal might be detectable in the highest frequency channel of the existing *BOOMERanG*³ data.

To calculate the correlation function, we must first understand the nature of the source(s) of the background. A compelling explanation is thermal emission by the interstellar dust of high-redshift galaxies, heated by their internal optical and ultraviolet (UV) star-light. A handful (~ 30) of sources with the expected properties have been resolved in several SCUBA images at $850\mu\text{m}$, reported in several papers (Hughes et al. 1998, Barger et al. 1998, Eales et al. 1999, Smail et al. 1997, Holland et al. 1998, Barger et al. 1999, Blain et al. 1999b) and summarized by Scott & White (1999), and another handful at $175\mu\text{m}$ with the ISOPHOT instrument on board the Infrared Space Observatory (ISO) (Puget et al. 1999). According to Hughes et al. (1998) and Barger et al. (1999), sources brighter than 2mJy comprise at least 25% of the background at $850\mu\text{m}$ (350 GHz). The observed source counts can be parameterized empirically by a softened power-law form (e.g. Barger et al. 1999). Using this form to extrapolate towards the faint end of the source count distribution (down to $\sim 0.5\text{mJy}$), one can account

¹*Planck*: <http://astro.estec.esa.nl/SA-general/Projects/Planck/>

²*TopHat*: <http://topweb.gsfc.nasa.gov>

³*BOOMERanG*: <http://www.physics.ucsb.edu/~boomerang>

for the entire background. These conclusions are further supported by the somewhat less reliable detections of faint sources down to $\sim 1\text{mJy}$. One should bear in mind, however, that such extrapolations are highly sensitive to the properties of the high- z population.

The sources identified by SCUBA are possibly galaxies. Two have been conclusively identified as such (Frayser et al. 1998). Hughes et al. (1998), observing in the Hubble Deep Field (HDF), identified tentative optical star-burst galaxy counterparts for all five of their sources brighter than 2mJy ; four of them with redshifts between 3 and 4 and one with $z \simeq 0.9$. These identifications are not yet conclusive, due to the coarse angular resolution of SCUBA, and the possibility remains that many of the sources are dust-enshrouded quasars, rather than galaxies (see, e.g. Sanders 1999).

It is also not yet clear that the FIRB is entirely due to the type of sources seen with SCUBA. Other possibly significant contributors include emission from inter-galactic dust, ejected from galaxies by radiation pressure or supernova winds (Aguirre 1999, Aguirre & Haiman 1999), numerous low surface brightness, dusty protogalaxies, and, more speculatively, radiatively-decaying massive particles (Bond, Carr & Hogan 1986). These contributions to the background will not be seen by experiments that are targeting relatively bright point sources. They would all, however, contribute not only to the mean level of the background, but also to its fluctuations on large angular scales, as long as their infrared emission traces the spatial mass fluctuations to some degree.

In this paper, we do not model the galaxy evolution process in any detail, but instead adopt a toy model that allows us to explore the dependence of the FIRB angular power spectrum on the nature of the sources, their redshift distribution, and cosmological parameters. More sophisticated models exist in the literature that generalize semi-analytical galaxy evolution schemes to make detailed predictions in the infrared regime (e.g. Toffolatti et al. 1998, Guiderdoni et al. 1998, Blain et al. 1999a). However, even these models are very much driven by the data and the semi-analytic approach has resulted in a wide range of predictions in the past. Here we choose a simplified approach, which is sufficient to illustrate the detectability of the clustering signals, their dependence on the large-scale distribution of matter and aspects of galaxy formation, and to demonstrate the need for further work.

An approach even simpler than our own is that of Scott and White (1996) who estimated the angular correlation function of the FIRB at $850\mu\text{m}$ by assuming that the FIRB sources have an angular correlation function like that of Lyman-break galaxies (Giavalisco et al. 1998). They viewed the FIRB as a contaminant of the CMB data, and were interested in a rough estimate of what these correlations might possibly be. As a result, they could ignore the fact that the projection effects would be different for the two different classes of objects. In the present paper, we investigate the FIRB as an interesting signal in its own right, and model it in sufficient detail to understand the dependence on large-scale structure and galaxy formation.

The spectra and correlation functions of both the near and far infrared backgrounds have been considered in general terms in the pioneering works of Bond, Carr & Hogan (1986, 1991). The recent measurements of the FIRB, the

discrete source detections discussed above, as well as determinations of the redshift-evolution of the global average star formation rate (e.g. Madau 1999 [M99]), the UV background at $z = 0$ (Bernstein 1997), and at $2 \lesssim z \lesssim 4$ (Giallongo et al. 1996) now allow a more focused discussion. When we calibrate our models using the recent infrared data, we find that the clustering results in contrasts of about 10% in the FIRB, which is sufficiently strong to dominate the shot-noise (estimated from the SCUBA detections) and to be detectable by proposed future missions. Jimenez & Kashlinsky 1997 have calculated the angular power spectra for the *near* infrared background, and also find contrasts of roughly 10%. Indeed, very recently, Kashlinsky et al. 1999 have claimed a tentative detection of fluctuations of cosmic origin in the DIRBE (Diffuse Infrared Background Explorer) maps from 1 to 5 microns, with the expected amplitude, or possibly slightly higher. The angular power spectrum in Scott and White (1996) is bracketed by those in our range of models, although most of our models tend to have somewhat higher amplitudes.

Our work has been strongly motivated by future missions including *Planck* and the *FIRBAT*. Both are capable of detecting these fluctuations, the *FIRBAT* by observing in eight channels with central wavelengths ranging from $230\mu\text{m}$ to $940\mu\text{m}$ with per-channel sensitivities between 25 and $130\mu\text{K s}^{1/2}$, and an angular resolution of $6'$. The broad range of frequencies is important for separating the FIRB fluctuations from those of dust in our own galaxy. It is possible that this signal is discernible in the existing *BOOMERanG* data, although the limited spectral coverage will make discrimination from dust in our own galaxy difficult.

The rest of this *Letter* is organized as follows. In § 2, we describe our toy model for the mean FIRB. In § 3, we extend this model to include the fluctuations, by assuming cold dark matter (CDM) power spectra, and that the FIRB light is a (biased) tracer of mass. In § 4, we show results in several models, including those with a uniform bias, and a redshift-dependent bias calculated according to a prescription for galactic halos (Mo & White 1996). In § 5, we discuss the results, and what can be learned from planned observations of the FIRB on large ($\gtrsim 5'$) angular scales, and finally in § 6, we summarize our conclusions.

2. MODELING THE MEAN FIRB

In our model, the FIRB arises from thermal dust emission. To compute the mean level of the flux, the main ingredients are the mass density Ω_d , and temperature T_d of dust, and the evolution of these quantities with redshift. The angular fluctuations depend further on the spatial distribution of the dust, as we will discuss in § 3 below. In order to compute the evolution of $\Omega_d(z)$ and $T_d(z)$, we rely on the recent determinations of the evolution of the global average star-formation rate (SFR, see Lilly et al. 1996, M99 and references therein). In particular, we assume that both the UV emissivity that determines the dust temperature, and the rate of dust production, are proportional to the global SFR (corrected for dust absorption), $\dot{\rho}_*(z)$, as given by M99. Our motivation for relying on the star-formation history is that the stellar UV flux is known to dominate that of quasars at all redshifts $z \lesssim 5$, with quasar contributions less than $\sim 20\%$ (M99). We assume further that the dust has a composition of 50% graphites

and 50% silicates by mass, and composite cross-sections as in the Milky Way (Draine & Lee 1984). Finally, we assume that the UV emissivity has the spectral shape obtained by summing individual zero-age main sequence stellar spectra weighted by a Scalo (1986) mass function (Bruzual & Charlot 1996).

[t]

TABLE 1

The parameter values in our standard model and its variants. The last two columns are the values of the dust density and temperatures at $z = 0$ (in Kelvin), determined from fitting the FIRB at $850\mu\text{m}$. See text for discussion.

	Ω_m	Ω_Λ	h	SFR	$T_{\text{Gr}}/T_{\text{Si}}$	Ω_d
Stand.	0.3	0.7	0.65	M99	14.4/10.1	2.7×10^{-5}
Open	0.3	0.0	0.65	M99	13.9/9.8	3.8×10^{-5}
SCDM	1.0	0.0	0.5	M99	14.1/9.9	5.4×10^{-5}
Flat	0.3	0.7	0.65	flat	17.1/12.9	3.5×10^{-5}
Hot	0.3	0.7	0.65	BSIK	40.0/40.0	2.0×10^{-6}
High- z	0.3	0.7	0.65	$z = 7$	12.9/9.1	2.9×10^{-5}

Under these assumptions, the dust temperature is determined by the UV radiation, i.e. by requiring that the amount of energy absorbed in the UV is equal to that thermally radiated in the infrared. The proportionality constants for the dust production rate and the UV emissivity are then determined by fitting the observed spectrum of the mean FIRB. The relevant equations are summarized in § 3 of Aguirre & Haiman (1999) (see also Loeb & Haiman 1997). Note that we have not assumed that the dust is perfectly uniformly distributed, but only that wherever there is dust, it is exposed to the same radiation field. Also note that in this scenario, as long as we are interested only in the mean level of the FIRB, we do not need to specify the spatial distribution of the dust, or the type of source from which the infrared emissivity arises. To get the angular power spectrum, we will assume below that dust is a (biased) tracer of mass on large scales (see § 3).

The parameters of our models are summarized in Table 1. Our standard model is a Λ CDM cosmology, with the SFR taken from M99. In this model, we find that in order to fit the FIRB, the graphite/silicate dust temperatures at $z = 0$ need to reach 14.4K and 10.1K, while the total mass density of dust has to reach $\Omega_d = 2.7 \times 10^{-5}$. The redshift evolution of these quantities are shown in the upper panel of Figure 1. In particular, Ω_d rises continuously as dust is accumulated from the increasing number of stars. The dust temperatures deviate from the CMB at $z \approx 7$, and stay roughly constant (silicates at $\sim 15\text{K}$, graphites at $\sim 25\text{K}$) until $z \sim 1$, at which point the SFR drops sharply, the dust heating becomes less efficient, and the dust temperatures start dropping again. The dust temperatures we obtain in our fiducial model at $z = 0$ are somewhat colder than, e.g. the temperature of dust in the Milky Way ($\sim 16 - 20\text{K}$, Reach et al. 1995). The temperatures are higher in our “flat” SFR model ($\sim 17/13\text{K}$, see Table 1 and discussion below), and are in better agreement with the Milky Way value. We therefore note that our conclusions are not dependent on an accurate reproduction of dust temperatures in local galaxies. In the lower panel of Figure 1, we show the redshift evolution of the comoving dust emissiv-

ity $j_d(z) = \rho_d \times \kappa_{d,\nu(1+z)} \times B_{\nu(1+z)}[T_d/(1+z)]$ in units of $10^{-21} \text{ erg cm}^{-3} \text{ s}^{-1} \text{ sr}^{-1} \text{ Hz}^{-1}$ at the (observed) wavelengths of $850\mu\text{m}$ (lower solid curve) and $450\mu\text{m}$ (lower dashed curve). Here κ is the dust opacity coefficient and B_ν is the Planck function. The curves in the figure illustrate the faster fall-off towards higher redshifts of the emissivity at $450\mu\text{m}$ compared to $850\mu\text{m}$, due to the fact that the peak of the grey body dust *observed* at $450\mu\text{m}$ occurs at lower z than for the longer wavelength $850\mu\text{m}$.

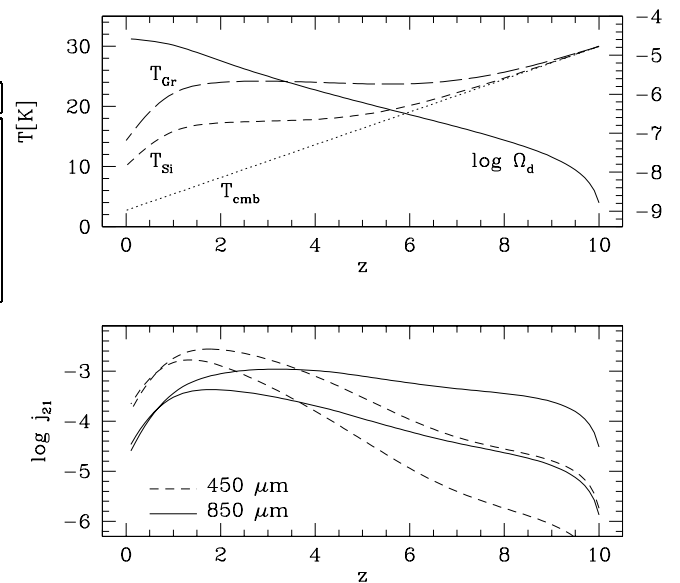


FIG. 1.— Upper panel shows the evolution of dust temperatures in our standard model, compared with the CMB temperature, as well as the mass density of dust. The labels on the right axis refer to $\log \Omega_d$. Lower panel shows the comoving dust emissivity j_d at $450\mu\text{m}$ and $850\mu\text{m}$ (bottom curves). The top curves show the quantity $b j_d$, where b is the bias parameter of galaxy sized ($10^{12} M_\odot$) halos.

We considered several variations on our standard model, summarized in Table 1. To explore the dependence of our results on the underlying cosmology, we have evaluated an open CDM model with $\Omega_m = 0.3$, and a standard CDM model. We then studied a “flat” SFR model, in which the SFR is constant in redshift. The motivation for considering this model is that the UV flux that heats the dust inside an individual galaxy may not evolve in the same way as the global average SFR does. Indeed, the evolution of the global SFR is driven mainly by the change in the number of galaxies, rather than the evolution of the characteristic brightness (Madau 1997). In this case, the dust temperature within each galaxy might stay roughly constant, provided it is heated by long-lived stars. To mimic this scenario, we have included a decreasing overall dust abundance according to the original M99 SFR, but set the UV emissivity to be a constant at all redshifts.

As an alternative to this scenario, we also considered a “hot” dust model, adopted from Blain et al. 1999c. In this model, the dust in each galaxy is kept hot by the more intense radiation from short-lived, intense bursts of star-formation, after which the dust cools down, and its emission is subsequently ignored. The total dust emission at a given redshift in this case is proportional to the UV emissivity, which, in turn, is proportional to the SFR.

Following Blain et al. 1999c, we assume a constant dust temperature of 40K, and a star-formation rate that is, in effect, a sum of the M99 SFR, and an additional Gaussian peak centered on redshift $z = 2.1$. Note that in this model, only a fraction of the total dust abundance is “luminous” at any given time – the entry for Ω_d in Table 1 refers to the maximum luminous dust density, reached at $z = 2.1$. Finally, we consider a “high- z ” variation on our standard model, in which we postulate an additional peak in the SFR at redshift $z = 7$, with $\text{SFR} \propto \exp[-(z-7)^2/2]$, and an amplitude such that this hypothetical high-redshift population accounts for 50% of the FIRB at $850\mu\text{m}$. The choice of this large burst of star formation is somewhat ad-hoc. Our motivation for considering this scenario is to characterize the possibility that the FIRB has a significant contribution from very high redshifts – an option that can not be ruled out by present observations. Note that significant star-formation at redshifts $z \gtrsim 5$ can still have escaped detection by, e.g., HST.

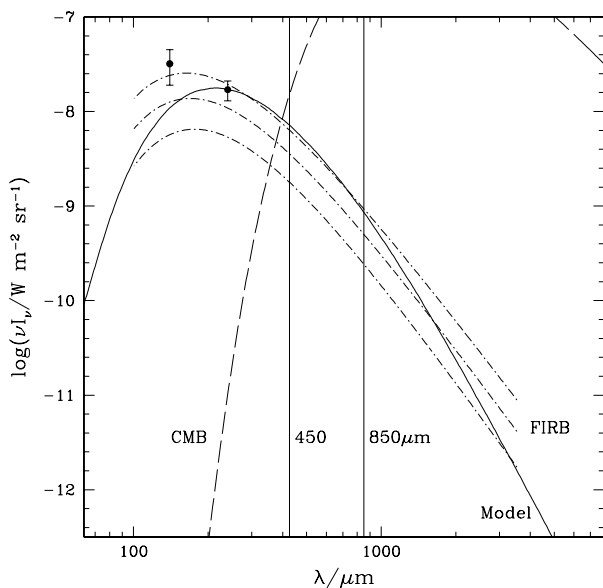


FIG. 2.— The spectrum of the FIRB predicted in our standard model (solid curve). The dot-dashed curves show the measurements with $\pm 1\sigma$ uncertainties from Fixsen et al. (1998), and the long dashed curves show the CMB for reference. The data-points are taken from Schlegel et al. 1998.

In Figure 2 we show the spectrum of the FIRB in our standard model. The dot-dashed curves show the fit to the measurements by Fixsen et al. (1998), while the solid line shows our model prediction. The long-dashed lines show the CMB, and the vertical solid lines mark the observational wavelengths of $450\mu\text{m}$ and $850\mu\text{m}$. As the figure reveals, the prediction from our model is in reasonably good agreement with the FIRB; in particular, it is within the quoted $\pm 1\sigma$ error bars. The quality of fits in the other models from Table 1 is similar to that of the standard model shown in Figure 2. The real sources of the FIRB are much more complex than our simplified model assumes. The UV flux density and the dust density are not expected to be spatially uniform, and dust in different galaxies could have different temperatures, broadening our predicted dust-emission peak. However, our model is sufficient to allow for a rough prediction for the angular

power spectra at various wavelengths, and to provide the framework for a discussion of what might happen with more realistic models.

3. FIRB FLUCTUATIONS

The model described so far accounts for the amplitude of the FIRB, but makes no specific reference to the spatial distribution of the infrared-emitting dust. In this section, we characterize the spatial distribution in order to derive the angular power spectrum of the FIRB. One simple assumption is that “dust traces mass”, i.e. that the local density of dust is proportional to the total mass density at every point in the universe. In reality, most of the dust could be confined in galactic halos; in which case the spatial distribution of dust emission would follow that of galactic halos. The correlation function of dark halos is related (Mo & White 1996) to that of mass by the bias parameter $b = b(M_{\text{halo}}, z)$. Here we adopt the modified formula of Jing (1999), which has been shown to reproduce the results of numerical simulations on a wider range of scales (including $M_{\text{halo}} < M^*$). Under these assumptions, the bias b is scale-independent for a fixed halo size, but evolves in redshift. The correlation function between pixels separated by angle θ and at frequencies ν and ν' is given by:

$$C^{\nu\nu'}(\theta) = \sum_l \frac{2l+1}{4\pi} C_l^{\nu\nu'} P_l(\cos \theta) \quad (1)$$

$$C_l^{\nu\nu'} = \frac{2}{\pi} \int k^3 P(k) f_{\nu l}(k) f_{\nu' l}(k) \frac{dk}{k} \quad (2)$$

$$f_{\nu l}(k) \equiv \int j_l(kr) b(r) D(r) j_d(\nu, r) a(r) dr \quad (3)$$

where $r \equiv c(\eta_0 - \eta)$ is the coordinate distance of an event at conformal time η on our past light cone, η_0 is the conformal time today, $P(k)$ is the power spectrum of the matter today, $a(r)$ is the scale factor normalized so that $a(0) = 1$, $D(r)$ is the linear theory growth factor, and j_l is the spherical Bessel function. In a matter-dominated universe, $D(r) = 1/a$. For the more general case of non-zero curvature and/or non-zero cosmological constant we use the fitting formula of Peebles (1980) and Carroll, Press & Turner (1992), respectively.

Equations 2 and 3 are a version of Limber’s equation (Limber 1953, Peebles 1980), although with power spectra instead of correlation functions and generalized to describe correlations between different components. Note that pixels at unequal frequencies will not be perfectly correlated because $j_d(\nu, z)$ and $j_d(\nu', z)$ are not proportional to each other for $\nu \neq \nu'$. The unequal-frequency correlation function (at $\theta = 0^\circ$, with $5'$ smoothing) has been calculated by Bouchet & Gispert (1999) by using simulated Planck maps generated using the semi-analytic model of Guiderdoni et al. (1998).

As equations (1-3) show, C_l scales roughly as b^2 . To illustrate the effect of a non-negligible bias, in the lower panel of Figure 1 we show the evolution of the comoving emissivity $j_d(\nu, z)$ at $450\mu\text{m}$ and $850\mu\text{m}$ (bottom curves), together with the quantity $j_d(\nu, z)b(M_{\text{halo}}, z)$ (top curves). We have assumed $M_{\text{halo}} = 10^{12} M_\odot$, which is valid if dust emission arises from dark halos of this size (roughly the size of galactic halos, as well as the host halos of typical

quasars, see Haiman & Loeb 1998). The figure shows that biasing significantly boosts the contribution to the signal from $z \gtrsim 1$, but has negligible effect at $z \lesssim 1$. In what follows, we alternately use this prescription for biasing and a time-independent bias of $b = 3$, which is roughly that of Lyman-break galaxies at $z \sim 3$ (Giavalisco et al. 1998).

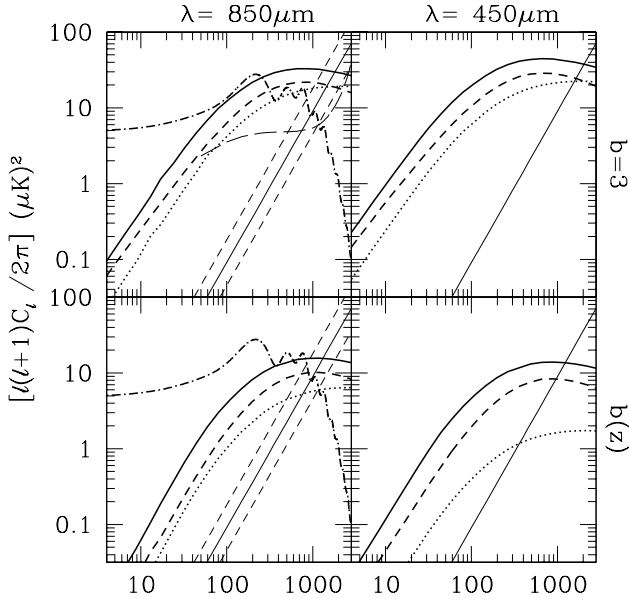


FIG. 3.— Predicted angular power spectra in units of $(\mu\text{K})^2$ (antenna temperature) for different cosmologies: ΛCDM (solid), SCDM (dashed) and OCDM (dotted), all assuming M99 SFR. The upper panels assume linear bias with a constant $b = 3$, and the lower panels assume a z -dependent bias. The left panels show the results at $450\mu\text{m}$ and the right panels at $850\mu\text{m}$. The long-dashed line on the upper left panel shows the sensitivity of *FIRBAT*, assuming bins of $\delta l = 50$ and a one week flight. For reference, the CMB power spectrum is also shown (dot-dashed lines in the $450\mu\text{m}$ panels). The light solid lines (with bounding dashes for the $450\mu\text{m}$ panels) are estimates of the shot-noise power with indications of the uncertainty. We do not attempt to characterize the uncertainty at $\lambda = 450\mu\text{m}$.

For our standard (ΛCDM) model, we have adopted the fitting formulae for the power spectrum given by Eisenstein & Hu (1999) with power-law index $n = 1$ and normalization $\sigma_8 = 1$, while in the Open and SCDM models, we used ($n = 1.3$, $\sigma_8 = 0.85$) and ($n = 0.7$, $\sigma_8 = 0.6$), respectively. These values for n and σ_8 were chosen to roughly agree with both the cluster abundance (Viana & Liddle 1999) and COBE-DMR (Bunn & White 1996) constraints. For the conversion between coordinate distance and scale factor for the ΛCDM model, we used the fitting formula of Pen (1999).

The total C_l is the sum of that due to correlations, which we have calculated, and that due to the discrete nature of the sources. This “shot-noise” C_l was calculated by Scott & White (1999) at $\lambda = 850\mu\text{m}$ who used the double-power law LF constrained by SCUBA data mentioned earlier and is shown in Fig. 3 rising like l^2 (as all white-noise power spectra do). The LF at $\lambda = 450\mu\text{m}$ is much more uncertain; we estimate the shot-noise at this wavelength simply by assuming that the *shape* of the LF is independent of frequency. Since the antenna temperature of the mean FIRB is roughly the same at these two wavelengths ($T_{\text{mean}} \simeq 60\mu\text{K}$), this means that the shot-noise at $450\mu\text{m}$ is the same as at $850\mu\text{m}$.

4. RESULTS

Our results are plotted in Figures 3 and 4. Figure 3 shows the predicted angular power spectra in units of $(\mu\text{K})^2$ (antenna temperature) for different cosmologies: ΛCDM (solid), SCDM (dashed) and OCDM (dotted), all assuming M99 SFR. The upper show our models with a constant linear bias $b = 3$, and the lower panels show models with a z -dependent bias. The left panels show the results at $450\mu\text{m}$ and the right panels at $850\mu\text{m}$. The long-dashed line on the upper left panel shows the sensitivity of *FIRBAT*, assuming bins of $\delta l = 50$ and a flight duration of 6×10^5 s. For reference, the CMB power spectrum is also shown (dot-dashed lines) in the $850\mu\text{m}$ panels. The light solid lines with bounding dashes in the same panels are estimates of the shot-noise power with indications of the uncertainty. We do not attempt to characterize the uncertainty at $\lambda = 450\mu\text{m}$. Figure 4 demonstrates how our results change due to variations away from our standard model (solid line): we show the flat SFR model (dotted), hot dust model (dashed), and high- z peak model (dot-dashed).

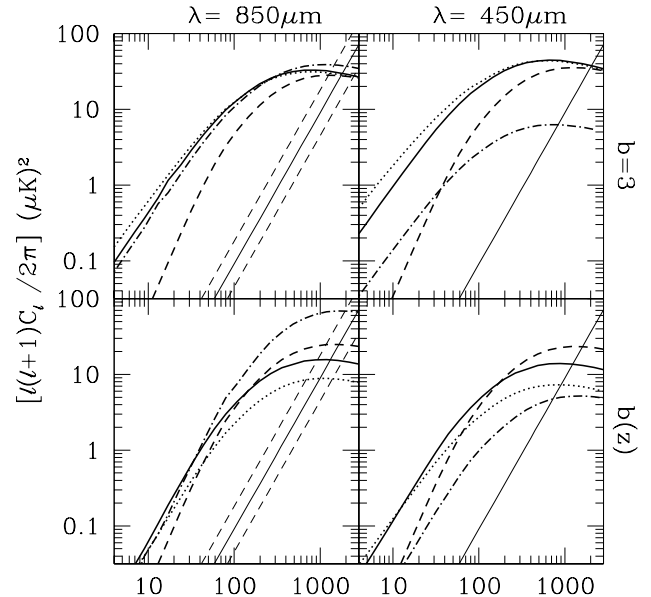


FIG. 4.— Angular power spectra as in Figure 3, but showing variations away from our standard model (solid line): flat SFR (dotted), hot dust (dashed), and high- z peak in SFR (dot-dashed).

The first thing to note is that the contrast ($\sqrt{l(l+1)C_l/(2\pi)}$) between $\ell \simeq 150$ and $\simeq 1000$ is about 10% of the $60\mu\text{K}$ mean and is mostly due to the intrinsic clustering of the FIRB, rather than shot-noise. We can roughly understand this basic result analytically with the following expression:

$$\frac{l(l+1)C_l}{2\pi} \sim T_{\text{mean}}^2 \left[\frac{b}{(1+z_{\text{peak}})} \right]^2 \Delta^2(k) \frac{\pi/k}{\sigma} \quad (4)$$

where $\Delta^2(k) \equiv k^3 P(k)/(2\pi^2)$ is the contribution to the variance of the matter density from each logarithmic interval in k , σ is the coordinate distance over which there is substantial emission, and $k \simeq l/r_{\text{peak}}$ where r_{peak} and z_{peak} are the coordinate distance and redshift of the peak emission. The right-most term is the inverse square of the

“wash-out factor” arising from the incoherent summing of structure at different redshifts, which reduces the contrast. Taking $z_{\text{peak}} \simeq 1$ and $l = 1100$ we find $k \simeq 0.5 h \text{Mpc}^{-1}$ and $\Delta^2(k) = 3$ for our standard model. Further taking $b = 3$ and $\sigma \simeq 3500 \text{ h}^{-1} \text{Mpc}$ we find $[\frac{l(l+1)C_l}{2\pi}]_{l=1100} \simeq 40 \mu\text{K}^2$. The shape of $l(l+1)C_l/(2\pi)$ (rising from low l , plateauing, and then slowly dropping) is due to a) the fact that $\Delta^2(k) \propto k^{3+n}$ at low k , flattening out to k^{n-1} at high k and b) the wash-out factor resulting in another factor of k^{-1} .

Note that the only quantities that matter for C_l are the matter power spectrum, $a(r)$, and the product $b(r)D(r)j_d(r)$. With the matter power spectrum and $a(r)$ fixed, any effect that pushes the bDj product to peak at higher redshifts, shifts the spectrum to higher l . Thus, for the constant bias cases, the flat SFR model has slightly more power at low l and the high- z SFR model is shifted to higher l . Likewise, the hot dust model has the steepest rise from low l to high l because its emissivity at both $450 \mu\text{m}$ and $850 \mu\text{m}$ rises from low z more quickly than any of the other models.

The redshift-dependent bias, $b(z)$, increases monotonically and at $z = 0, 2$ and 7 has values of $1, 3$ and 18 respectively. Because $b(z < 2) < 3$ the redshift-dependent bias generally decreases the fluctuation power compared to the $b = 3$, z -independent case. This is especially true at low l and also for $\lambda = 450 \mu\text{m}$. The exceptions are the high- z SFR case and the hot dust case at $\lambda = 850 \mu\text{m}$, due to the significant emission from $z > 2$.

5. DISCUSSION

Our simplified model of the sources is insufficient for many purposes, e.g., predicting the luminosity function, but is adequate for predicting the large-angular scale power to within factors of ~ 2 . The key assumption is that the dust-light is a biased tracer of the mass; i.e., where there is more mass there is proportionately more light. Note that in principle, a non-negligible fraction of the unresolved FIRB at $450 \mu\text{m}$, and especially at $850 \mu\text{m}$, could arise from the direct emission from optically faint quasars (Haiman & Loeb 1998); our approach would be equally applicable in this case. The fluctuation level of 10% is fairly model-independent, although linearly dependent on the bias of the sources. If the bias is unity, as is the case for galactic halos near $z \approx 0$ (Mo & White 1996), then the contrast may be as small as a few per cent.

Contrasts observed to be smaller than a few percent would be surprising. This would indicate that most of the FIRB comes from sources with $b \lesssim 1$, so that $b(r)D(r)$ is small where $j(r)$ is large. Examples of such sources would be galaxies near $z \approx 0$, or intergalactic dust at high redshifts. The former case might be difficult to reconcile with the relatively low number of nearby IRAS sources. In the latter case, one would need to invoke dust temperatures higher than expected based on the estimates of the UV background (Bernstein 1997), in order to get the correct spectrum for the mean FIRB in the full $150 - 1000 \mu\text{m}$ range (Aguirre & Haiman 1999).

The correlated component can even be measured on angular scales where it is smaller than the shot-noise. The shot-noise contribution can be reduced by observing at

high resolution and masking out pixels with fluxes above some threshold. Fluctuation analyses of point-source cleaned SCUBA maps have been done by two groups (Hughes et al. 1998, Borys, Chapman & Scott 1998). However, at these sub-arcminute angular scales, the wash-out factor is very large, and the correlated component is expected to be very small. These analyses were motivated by the desire to see the shot-noise due to unresolved sources below the flux cut, and resulted in constraints on the faint-end slope of the number counts.

An actual detection of the FIRB fluctuations will be highly valuable. The spectrum of the FIRB *anisotropy* may eventually be better known than the spectrum of the FIRB *mean* due to the experimental advantages of differential measurements. Such an improved determination of the FIRB spectrum would provide detailed constraints on galaxy formation models, in addition to those from the amplitude and scale-dependence of the anisotropy signal. It will also be interesting to examine the cross-correlations of the FIRB fluctuations with other data such as the CMB (FIRB sources may lens the CMB, or both backgrounds may be lensed by the same mass distributions), radio sources (from, e.g., the FIRST VLA survey or the MAP⁴ 22 GHz channel), galaxies, or quasars at different redshift slices from the 2dF (e.g., Folkes et al. 1999) and Sloan Digital Sky Survey (SDSS, see e.g., Gunn & Weinberg 1995), and the X-ray, and near infrared backgrounds (the same sources could contribute to the backgrounds at both of these wavelengths).

Further development of predictions for the statistical properties of the FIRB is clearly warranted. The correlation function, the statistical property we have focused on here, may prove easier to understand than the luminosity function—the bright end of which is probably dominated by very rare events (Bond 1999). Correlation function predictions will be refined by detailed modeling that is informed by additional observations. One useful input will be the clustering properties of galaxies and quasars, measured accurately in forthcoming redshift surveys, such as 2dF and SDSS. It may then be possible to infer the nature of the sources of the FIRB by comparing its statistical properties to those of galaxies and quasars.

In the preceding, we have implicitly assumed that the large-scale distribution of matter ($P(k)$ and its evolution with redshift) will have been determined by high-precision CMB anisotropy measurements and redshift surveys, and have therefore been focusing on the dependence of C_l on the nature of the sources. However, we emphasize that the FIRB C_l is sensitive to large-scale structure at redshifts intermediate to those that will be directly probed by these redshift surveys ($z \lesssim 1$) and CMB missions ($z \simeq 1100$). It will also be sensitive to wavelengths too small to be constrained by the CMB measurements, and at any given comoving wavelength the matter fluctuations will be better approximated by linear theory than they are at lower redshifts. The relation of C_l to large-scale structure is complicated by its simultaneous dependence on $j_d(\nu, z)$ and the bias properties of the sources, but these complications will be reduced both by improved theoretical modeling of the sources and also by high-resolution, deep observations, together with identification of counterparts at other wave-

⁴ MAP: <http://map.gsfc.nasa.gov>

lengths. Thus we view point source observations and measurements of fluctuations on large angular scales as complementary: the recovery of the power spectrum on large scales from C_l observations is aided by measurement of the point sources, which is incapable of determining the power spectrum alone.

6. CONCLUSIONS

The recently discovered cosmic Far Infrared Background and the galaxy counts at $850\mu\text{m}$ have opened a new wavelength at which galaxy formation and evolution and large-scale structure can be studied empirically. A significant fraction of the FIRB has already been resolved by SCUBA into discrete sources; however, due to the lack of detailed spectral information, identified counterparts in other bands, and secure redshift determinations (except for the two sources in Frayer et al. 1998), fundamental questions still remain unanswered. Does the population of the observed sources indeed account for the full background? What is the nature of the observed sources: are they galaxies, dust-enshrouded AGN, or a mixture of both? What are their redshift distributions? We have

argued that measurements of the FIRB correlation function can help answer these questions and also that the FIRB provides a unique probe of the large-scale distribution of matter at intermediate redshifts. We have found that under simple, but broad, models for the mean FIRB, the anisotropy of the unresolved FIRB intensity is at the 3 to 10 percent level. These fluctuations are measurable with proposed balloon-borne instruments and future space missions whose datasets will add new, useful constraints on large-scale structure and models for the formation and evolution of galaxies and quasars.

We thank the TopHat group, and G. Wilson in particular, for asking what could be learned from observing FIRB anisotropy, J. R. Bond, S. S. Meyer and D. N. Spergel for useful conversations, P. Madau for providing a fitting formula for the SFR, and the referee, A. Blain, for a careful reading of the manuscript and useful comments. LK is supported by the DOE, NASA grant NAG5-7986 and NSF grant OPP-8920223. ZH was supported by the DOE and the NASA grant NAG 5-7092 at Fermilab.

REFERENCES

- Aguirre, A. 1999, ApJ, in press, preprint astro-ph/9904319
 Aguirre, A., & Haiman, Z. 1999, ApJ, submitted, preprint astro-ph/9907039
 Barger, A. J., Cowie, L. L., Sanders, D. B., Taniguchi, Y. 1998, Nature, 394, 248
 Barger, A. J., Cowie, L. L., & Sanders, D. B., 1999, ApJ, 518, L5
 Barger, A. J., Cowie, L. L., Smail, I., Ivison, R. J., Blain, A. W., & Kneib, J.-P. 1999, AJ, 117, 2656
 Bernstein, R. 1997, PhD Thesis, Caltech
 Blain, A. W., Ivison, R. J., & Smail, I. 1998, MNRAS, 296, L29
 Blain, A. W., Jameson, A., Smail, I., Longair, M. S., Kneib, J.-P., & Ivison, R. J. 1999a, MNRAS, submitted, preprint astro-ph/9906311
 Blain, A. W., Kneib, J.-P., Ivison, R. J., & Smail, I. 1999b, ApJ, 512, L87
 Blain, A. W., Smail, Ivison, R. J., & Kneib, J.-P. 1999b, MNRAS, 302, 632 [BSIK]
 Bond, J. R., personal communication, 1999.
 Bond, Carr, & Hogan 1986, ApJ, 306, 428
 Bond, J. R., Carr, B. J., & Hogan, C. J. 1991, ApJ, 367, 420
 Borys, C., Chapman, S. C., & Scott, S. 1998, MNRAS, submitted, preprint astro-ph/9808031
 Bouchet, F.R., & Gispert, R., 1999, astro-ph/9903176.
 Bruzual, G., & Charlot, S. 1996, in preparation. The models are available from the anonymous ftp site gemini.tuc.noao.edu.
 Bunn, E., & White, M. 1997, ApJ, 480, 6
 Carroll, S. M., Press, W. H., Turner, E. L. 1992, ARA&A, 30, 499
 Dragovan, M., space mission concept presented at the David N. Schramm Memorial Symposium: Inner Space / Outer Space II, Batavia, IL.
 Draine, B. T., & Lee, H. M. 1984, ApJ, 285, 89
 Dwek, E., et al. 1998, ApJ, 508, 106
 Eales, S., Lilly, S., Gear, W., Dunne, L., Bond, J. R., Hammer, F., Le Fevre, O., & Crampton, D. 1999, ApJ, 515, 518
 Eisenstein, D. J., & Hu, W. 1999, ApJ, 511, 5
 Fixsen, D. J., et al. 1998, ApJ, 508, 123
 Folkes, S. et al. 1999, astro-ph/9903456
 Frayer, D. T., Ivison, R. J., Scoville, N. Z., Yun, M., Evans, A. S., Smail, I., Blain, A. W., Kneib, J.-P., 1998, ApJ, 506, 7
 Giallongo, E., Cristiani, E., D'Odorico, S., Fontana, A., & Savaglio, S. 1996, ApJ, 466, 46
 Giavalisco, M., Steidel, C. C., Adelberger, K.L., Dickinson, M. E., Pettini, M., Kellogg, M., 1998, ApJ 503, 543 [astro-ph/9802318].
 Guiderdoni, B., Hivon, E., Bouchet, F. R., & Maffei, B. 1998, MNRAS, 295, 877
 Gunn, J. E., & Weinberg, D. H. 1995, in *Wide-Field Spectroscopy and the Distant Universe*, ed. S. J. Maddox and A. Aragon-Salamanca (Singapore: World Scientific), 3
 Haiman, Z., & Loeb, A. 1998, ApJ, 503, 505
 Holland, W. S., et al. 1998, Nature, 392, 788
 Hughes, D., et al. 1998, Nature, 398, 241
 Jimenez, R., & Kashlinsky, A. 1997, ApJ, 511, 16
 Jing, Y. P. 1999, ApJ, 515, L45
 Kashlinsky, R., Mather, J. C., Odenwald, S., 1997, astro-ph/9701216
 Kashlinsky, R., Mather, J. C., Odenwald, S., 1999, ApJ, in press, astro-ph/9908304
 Lagache, G., Abergel, A., Boulanger, F., Désert, F. X., Puget, J.-L. 1999, A&A, 344, 322
 Lilly, S. J., Le Fevre, O., Hammer, F., & Crampton, D. 1996, ApJ, 460, L1
 Limber, D. N. 1953, ApJ 117, 134
 Loeb, A., & Haiman, Z. 1997, ApJ, 490, 571
 Madau, P. 1997, in *Star Formation Near and Far : Seventh Astrophysics Conference*, Eds. Steven S. Holt and Lee G. Mundy, Woodbury N. Y. : AIP Press; AIP Conf. Ser., 393, 481
 Madau, P. 1999, in *Physica Scripta*, Proc. of the Nobel Symposium "Particle Physics and the Universe", held at Enköping, Sweden, August 20-25, 1998, in press, preprint astro-ph/9902228 [M99]
 Mo, H. J., & White, S. D. M. 1996, MNRAS, 282, 347
 Peebles, P. J. E. 1980, *Large-Scale Structure of the Universe*, Princeton Univ. Press
 Pen, U.-L. 1999, ApJS, 120, 49
 Puget, J. L. et al. 1996, A&A, 308, L5
 Puget, J. L. et al. 1999, A&A, in press, astro-ph/9812039
 Reach, W. T. et al. 1995, ApJ, 451, 188
 Sanders, D. B. 1999, in Proc. of IAU Symposium No. 194, "Activity in Galaxies and Related Phenomena", in press, preprint astro-ph/9903445
 Smail, I., Ivison, R. J., & Blain, A. W. 1997, ApJ, 490, L5
 Scalo, J. M. 1986, *Fundamentals of Cosmic Physics*, 11, 1
 Schlegel, D.J., Finkbeiner, D. P., Davis, M., 1998, ApJ 500, 525
 Scott, D. & White, M. 1999, A&A, 346, 1
 Toffolatti L., Argüeso Gomez, F., De Zotti, G., Mazzei, P., Franceschini, A., Danese, L., & Burigana, C., 1998, MNRAS, 297, 117
 Viana, P. T. P., & Liddle, A. R. 1999, MNRAS, 303, 535
 Vogeley, M. S. 1997, ApJ, submitted, preprint astro-ph/9711209